

# Changes induced by electrochemical oxidation of poly(9,9-dioctylfluorene-*alt*-thiophene): towards a correlation between charge transport, molecular structure modifications and degradation

Camila Gouveia Barbosa<sup>1</sup> · Danielly Cristina Bento<sup>2</sup> · Laura Oliveira Péres<sup>1</sup> · Guy Louarn<sup>3</sup> · Henrique de Santana<sup>2</sup>

Received: 10 March 2016 / Accepted: 30 May 2016 / Published online: 3 June 2016  
© Springer Science+Business Media New York 2016

**Abstract** In this work, an alternating copolymer of fluorene and thiophene, the poly(9,9-dioctylfluorene-*alt*-thiophene) (PDOF-*alt*-Th), was synthesized by the Suzuki coupling reaction. To confirm its molecular structure, the copolymer was characterized by means of photoelectron, vibrational and optical spectroscopies. Raman scattering and infrared absorption spectra were fully interpreted, with the support of DFT modeling. It was found that the incorporation of thiophene units along the poly(9,9-dioctylfluorene) chain caused a red shifted emission, and thus the UV–Vis spectroscopy was also used to determine the value of the optical band gap and electron affinity. Electrochemical and electrical properties were then investigated by means of cyclic voltammetry (CV) and electrochemical impedance spectroscopy (EIS). The values of ionization potential ( $I_p$ ) and the charge transfer resistance ( $R_{CT}$ ) at different potentials were determined. The EIS results showed an increase of conductivity at the first oxidation potential peak of the compound which was related with the formation of the thiophene radical cation. Consequently, the electroactive behavior of the copolymer was complemented by means of UV–Vis *ex situ* and Raman-spectroelectrochemical analysis. Finally, electrical, electrochemical and optical changes induced by electrochemical oxidation were presented, and the relationship

between molecular structure modifications and charge generation are discussed.

## 1 Introduction

Studies of  $\pi$ -conjugated polymers that are potentially applied in organic solar cells and organic light-emitting diode have been intensively reported in the literature since 15 years [1–4]. The ability to modify their chemical structure, good processability, innovative optical properties and the relative low cost of these organic materials justify this large interest of the scientific community. In this field, polyfluorenes (PFs) and its derivatives have proved to be a good candidate in the organic electronic applications, considering their efficient luminescence combined with high mobility and stability [5].

There are several methods of preparing polymeric semiconductors. One of them, which became very popular in the last decade, is the synthesis of alternating copolymers consisting of electron donating and electron accepting units [6]. These copolymers can be prepared from appropriate building blocks using different types of C–C coupling reactions [6–8]. Thus, different polyfluorene alternating copolymers have been studied and their performances as active matter in organic light-emitting diodes (OLEDs), organic field effect transistors (OFETs), chemical sensors or in organic photovoltaic cells can be found in the scientific literature [3–5]. All these applications require strict control of the polymer redox properties (more precisely, the positions of the HOMO and LUMO energy levels) which must be adapted to a given application. This makes the synthesis of new electroactive polymers a challenging task. For instance, fluorene containing organic photosensitizers, donor–acceptor alternating copolymers

✉ Henrique de Santana  
hensan@uel.br

<sup>1</sup> Laboratory of Hybrid Materials, Federal University of São Paulo, Diadema, São Paulo, Brazil

<sup>2</sup> Departamento de Química, CCE, Universidade Estadual de Londrina, 86051-990 Londrina, Paraná, Brazil

<sup>3</sup> Institut des Matériaux Jean Rouxel, Université de Nantes-CNRS, 44322 Nantes, France

containing fluorene or alternating conjugated copolymers consisting of fluorene and thiophene groups, have been studied due to their promising optical and electrochemical properties [9–12].

This study aimed to evaluate the electrical and optical properties of poly(9,9-dioctylfluorene-*alt*-thiophene) synthesized by Suzuki coupling reaction [13]. Any application of this polymer requires its detailed physicochemical characterization. This involves the elucidation of the polymer chain microstructure by spectroscopic techniques (NMR, FTIR and other techniques), the determination of their macromolecular parameters such as molecular mass and its distribution. Such investigations have been undertaken using FTIR, Raman, UV–Vis–NIR absorption and photoelectron spectroscopies (XPS). As vibrational spectroscopies (Resonance Raman scattering and infrared absorption) have become powerful tools for obtaining structural information in conjugated polymers, assignments of characteristic Raman and infrared peaks were critically discussed. Also, UV–Vis absorption and emission spectra have been investigated, which provide complementary information and allow the determination of the HOMO and LUMO levels. In addition, the study of the conductive process in organic materials is important for understand the factors that influence their electronic properties and its applications. A detailed electrochemical characterization of the synthesized compounds is presented which involves cyclic voltammetry (CV) and electrochemical impedance study (IES). Especially, CV was used to understand the electroactive material behavior, and EIS has been used as an alternative for the determination and understanding of electrical parameters such as charge transfer resistance in a wide frequency band [14–16]. Finally, Raman spectro-electrochemistry was investigated, in order to understand the influence of the potential applied to the film deposited on platinum, especially in the charge transfer process observed in the Nyquist diagrams. From these results, a local description of the charge carriers on the copolymer chain was suggested.

## 2 Experimental

### 2.1 Copolymer synthesis

The copolymer poly(9,9-dioctylfluorene-*alt*-thiophene) was synthesized according to literature [13, 17]. The procedure can be briefly described as follows (see scheme 1). In a reflux system, 2.62 mmol of 9,9-dioctylfluorene-2,7-diboronic acid (Aldrich, 96 %), 2.12 mmol of 2,5-dibromothiophene (Aldrich, 95 %), 0.013 mmol of tetrakis(triphenylphosphine) palladium ( $\text{P}(\text{Ph}_3)_4\text{Pd}$ ) (Aldrich, 99 %) as catalyst, were dissolved in 120 mL of xylene, and

10 mL of 2 mol/L of potassium carbonate. This solution was stirred for 72 h at 100 °C under nitrogen flow (step 1). Thereafter, 0.5 mmol of 2-bromothiophene (Aldrich, 98 %) was added and then kept under reflux for 24 h (step 2). Finally, 20 mL of hydrogen peroxide were slowly added. It should be noted that all organic materials were firstly extracted with toluene, and the polymer was recrystallized with methanol (yield 97 %). Characterization data:  $^1\text{H}$  NMR (400 MHz,  $\text{CDCl}_3$ ,  $\delta$ , ppm): 7.64, 7.61, 7.55, 7.35, 7.28, 7.19, 7.05, 2.55, 2.25, 2.00, 1.51, 1.18, 1.03, 0.73.  $^{13}\text{C}$  NMR (400 MHz,  $\text{CDCl}_3$ ,  $\delta$ , ppm): 124.64, 123.92, 120.15, 119.82, 40.49, 31.81, 30.04, 29.23, 23.78, 22.61, 14.09.  $^{13}\text{C}$  NMR (400 MHz, solid state)  $\delta$ : 152.9, 145.3, 142.1, 134.6, 125.4, 122.8, 56.9, 42.8, 31.6, 24.6 and 15.82 IR ( $\text{cm}^{-1}$ ): 3066, 3025, 3004, 2950, 2921, 2866, 2848, 1606, 1460, 1417, 1260, 1090, 1017, 880, 813, 794 and 720. Raman ( $\text{cm}^{-1}$ ): 1606, 1587, 1490, 1446, 1361, 1278, 1133 and 1078.

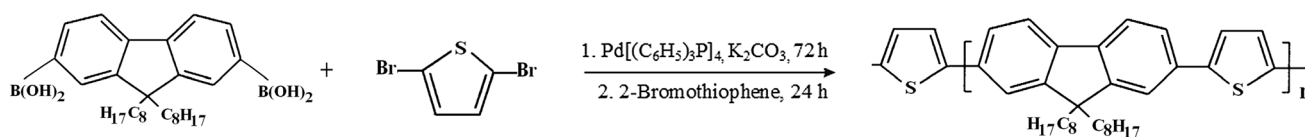
### 2.2 Characterization

UV–Vis absorption spectra were collected on a Shimadzu 1501 spectrophotometer. The copolymer was dissolved in chloroform, and the solutions were poured into 10 mm square quartz cells. The photoluminescence (PL) spectra were obtained with a Shimadzu 5301PC, slit width 5 mm; the wavelengths of the maximum absorption according to the UV–Vis spectra were used as the excitation wavelengths. UV–Vis reflectance data were obtained using a UV–Vis spectrophotometer (Shimadzu) coupled to an ISR-2600 integrating sphere.

Raman spectra of neutral copolymers was recorded on a WITec alpha 300 s spectrometer ( $\lambda_{\text{exc}} = 785$  nm, 10  $\mu\text{m}$  diameter spot, typical exposure times 10 min). Fourier-transform infrared (FT-IR) spectra were acquired on a Shimadzu IR Prestige-21 at a spectral resolution of 4  $\text{cm}^{-1}$  in the frequency range 4000–500  $\text{cm}^{-1}$ ; the samples were compacted into KBr pellets.

XPS measurements were carried out at room temperature with an Axis Nova spectrometer from Kratos Analytical with Al  $\text{K}\alpha$  line (1486.6 eV) as the excitation source. Thin layers of polymers were deposited on a glass substrate from chloroform solutions by drop-casting, then dried under a gentle nitrogen flux, then directly introduced overnight in the sample exchange chamber of the spectrometer. Survey spectrum was acquired at pass energy of 80 eV and with an energy step of 1 eV. The core level spectra (C 1s, O 1s, and N 1s) were acquired using a constant pass energy mode of 20 eV, (energy resolution of 0.48 eV). Concerning the calibration, binding energy for the C 1s hydrocarbons peak was set at 284.8 eV.

Cyclic voltammetry (CV) registered for thin polymer films drop-cast onto a platinum electrode, with a



**Scheme 1** Synthesis of copolymer poly(9,9-dioctylfluorene-*alt*-thiophene)

potentiostat/galvanostat device, model Autolab PGSTAT 302 N, coupled to the computer with NOVA 1.8 software. The experiments were carried out in a one compartment electrochemical cell, in a solution of 0.100 mol.L<sup>-1</sup> LiClO<sub>4</sub> in acetonitrile (ACN), with a silver chloride electrode (Ag/AgCl) as reference and a Pt plate as counter electrode. Electrochemical Impedance diagrams conducted at different potentials were obtained using the Autolab potentiostat PGSTAT 302 C with FRAM32 impedance module, varying the frequency from 100 kHz to 0.01 Hz. The measurements were started after waiting 5 min. This is necessary to achieve the steady state wherein the current was constant. The in situ Raman spectra were obtained from the portable Raman spectrometer Advantage532<sup>®</sup> of DeltaNu, ( $\lambda_{\text{exc}} = 532 \text{ nm}$ , 8 cm<sup>-1</sup> resolution). The NuSpec DeltaNu software was used, using baseline features to remove background fluorescence. During the Raman acquisition, the potentials were applied using a potentiostat equipment. After each potential raise, a wait time was applied until the *quasi*-equilibrium state was reached, then the Raman spectrum was registered “in situ”. It was assumed that the equilibrium state was reached when the potential change induced current became negligible.

NMR spectra were obtained on a Bruker spectrometer Model Avance III operating at 400 MHz for <sup>1</sup>H and 100 MHz for <sup>13</sup>C using a 5 mm broadband probe. NMR resonances were registered using CDCl<sub>3</sub> as solvent and TMS as internal standard. Chemical shifts ( $\delta$  in ppm) were referenced to the residual solvent signal (CHCl<sub>3</sub> in CDCl<sub>3</sub> at  $\delta$  7.24). Solid state <sup>13</sup>C spectra (<sup>13</sup>C CP MAS NMR) were recorded on a Bruker (Avance III) instrument operating at 400 MHz. A multinuclear probe (4 mm) and a zirconium oxide rotor were used with a cross polarized-magic angle spinning (CP-MAS) unit.

### 2.3 Modeling

The vibrational frequencies of PDOF-*alt*-Th were calculated using a commercial program package, Gaussian09 package [18]. Calculations were performed using the B3LYP functional together with a 6-31++G (d,p) basis set. The first geometry optimizations determined the most stable conformers of each sequence of polymers. After, theoretical frequencies were calculated. No negative frequencies were encountered. It should be noted that computed frequency values contain known systematic errors

resulting in overestimates. Therefore, it is usual to scale the theoretically predicted frequencies by an empirical factor. In the case of PDOF-*alt*-Th, the theoretical frequencies were scaled by a factor of 0.959 (frequency under 1700 cm<sup>-1</sup>) or 0.944 (frequency > 2800 cm<sup>-1</sup>), which were obtained by normalizing the theoretical value to the experimental value for the “Out of plane” bending CH (thiophene) modes and the CH stretching mode (experimental 794 and 2921 cm<sup>-1</sup>, theoretical 828 and 3096 cm<sup>-1</sup> respectively). It should be stressed that the calculations here presented were performed in vacuum, on an isolated chain segments. However, thanks to reasonable agreement between the experimental and calculated frequencies, considerably more expensive quantum chemical calculations were estimated unnecessary. The vibrational modes were assigned by means of visual examination of cartesian displacements of the modes using the GaussView program.

### 3 Results and discussion

The chemical structures of the studied copolymers are depicted in Scheme 1. In order to confirm their molecular structure, but also to check that no degradation or partial oxidation took place during the drop-casting method, FTIR, Raman and XPS experiments on as prepared compounds were first conducted.

To elucidate the molecular structure of pristine copolymer, we present in the Figs. 1 and 2 the results of quantum chemical calculations and the data obtained by vibrational spectroscopies. It is well known that all features of infrared absorption and Raman scattering spectra are signatures of the molecular structure since they are determined by the conformation of the molecule (macromolecule) and the distribution of the valence electron density. However, in this approach the main difficulty is often to find the attribution of the Raman and IR peaks, and then to interpret these complex spectroscopic data in terms of molecular structure. Therefore, the support of quantum chemistry calculations is frequently needed.

In Figs. 1 and 2, FT-IR and Raman spectra and modeling of the studied copolymer are shown. The calculated spectrum consisting of Lorentzian-shape peaks (Figs. 1a, 2a) is compared with the experimental one (Fig. 1b, 2b). The width of the Lorentzian lines has to be adjusted to approximate the appearance of the actual spectra (the

**Fig. 1** Infrared absorption spectra of pristine PDOF-*alt*-Th: **a** computed infrared absorption spectrum, **b** experimental infrared absorption spectrum

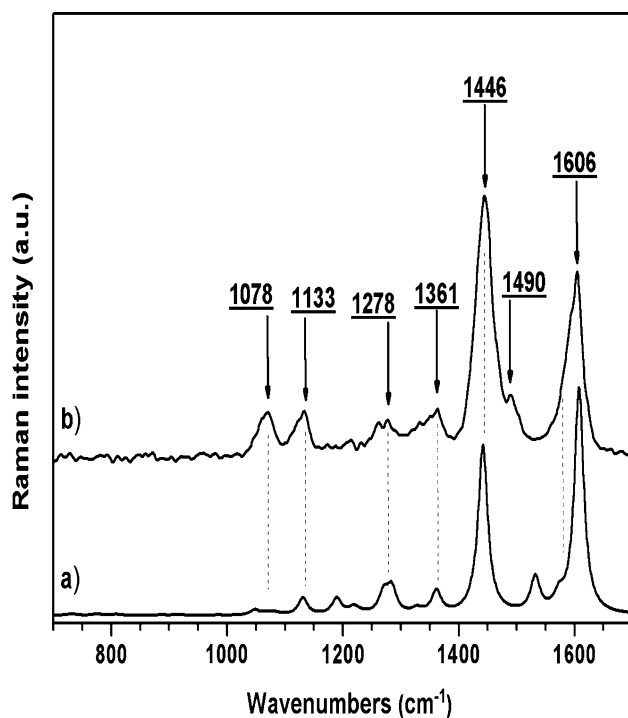
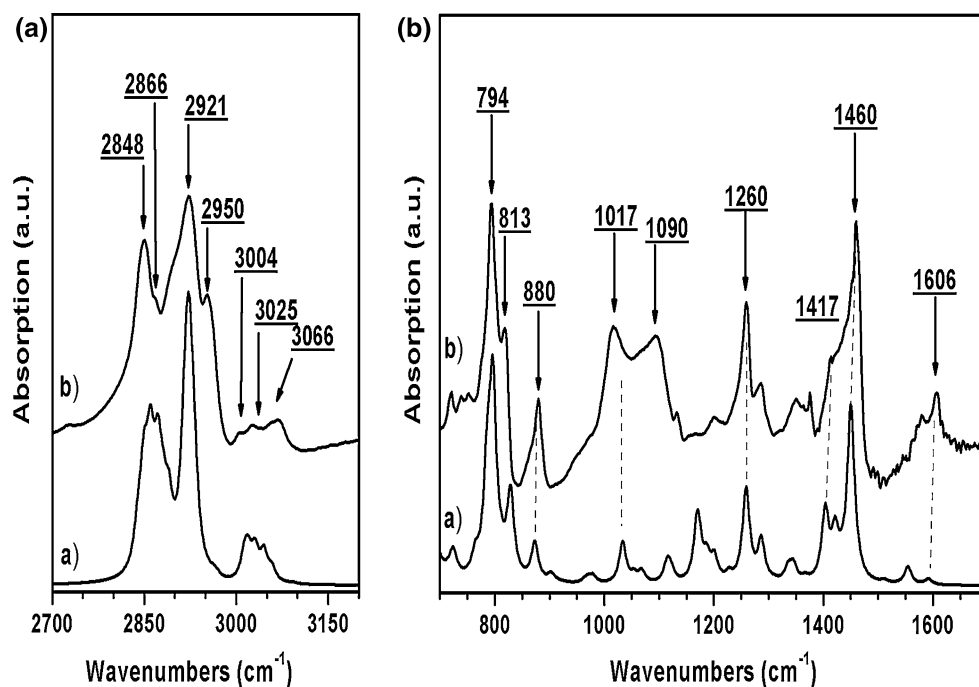


**Fig. 2** Raman scattering spectra of PDOF-*alt*-Th: **a** simulated Raman spectrum, **b** experimental Raman scattering spectrum (thin film,  $\lambda_{\text{exc}} = 785 \text{ nm}$ )

*FWHM* was set to  $8 \text{ cm}^{-1}$  for Raman and infrared absorption spectra). Despite the fact that the DFT calculations were performed in the gas-phase environment, which should be considered as a rough assumption, the

agreement with the experimental data was good enough for assignments and to understand the spectroscopic data.

The attributions of vibrational modes of the studied polymer, listed in Table 1 (infrared absorption and Raman scattering peaks) were done with the support of previous publications, [19–22] appropriate reference book [23] and exploiting the DFT modeling. The results presented in this table are largely self-explanatory, so the discussion is limited to the main observed bands (experimentally).

Concerning the infrared spectrum, the most intense bands at 3055, 1430, 1375, 1201, 1017, 794 and  $720 \text{ cm}^{-1}$  were assigned to the thiophene ring [19]. The bands at 2960, 2920, 2848, 1430 and  $1350 \text{ cm}^{-1}$  was due to the saturated hydrocarbons ( $\text{C}_8\text{H}_{17}$ ). Finally, peaks at 3025, 3004, 1606, 1417, 1260, 1090 and  $880 \text{ cm}^{-1}$  were related to the fluorene aromatic group [24]. According to the literature, the bands at 880, and  $813 \text{ cm}^{-1}$  indicate the presence of the 1,2,4-trisubstituted aromatic ring of the poly(9,9-dioctylfluorene) [23]. The frequencies at 795 and  $1018 \text{ cm}^{-1}$  were assigned to CH deformation out-of-plane and in the plane, respectively, in positions 3 and 3' of thiophene disubstituted ring which can be considered that the thiophene rings have been condensed between fluorene rings, according to the scheme 1. Thus, the coexistence of features bands of poly(9,9-dioctylfluorene) (PDOF) and thiophene (Th) confirm the formation of the poly(9,9-dioctylfluorene-*alt*-thiophene) copolymer.

In a similar manner, careful inspection of the Raman data was presented in Table 1. The most characteristic features of the calculated and registered Raman spectra can

**Table 1** Experimental and calculated frequencies (in  $\text{cm}^{-1}$ ) of the main vibrational modes of PDOF-*alt*-Th

PDOF- <i>alt</i> -Th				Assignments
IR abs.		Raman bands		
Expt.	Calc.	Expt.	Calc.	
3055	3056			CH sym. stretching thiophene ring
3050	3050			CH asym. stretching thiophene ring
3025	3030			CH sym. stretching fluorene ring
3004	3018			CH asym. stretching fluorene ring
2950	–			CH asym. stretch ( $\text{CH}_3$ )
2921	2924			CH asym. stretch ( $\text{CH}_2$ )
2866	2874			CH sym. stretch ( $\text{CH}_3$ )
2848	2862			CH sym. stretch ( $\text{CH}_2$ )
1606	1592	1606	1608	C=C stretch (fluorene ring)
1579	1555	1587	1578	C=C stretch (fluorene ring)
		1490	1531	C=C asym. stretch (fluorene ring)
1460	1449			C=C sym. stretch + CH bend (fluorene ring)
1430	1422	1446	1446	C=C stretch (thiophene ring) + bending $\text{CH}_2/\text{CH}_3$
1417	1404			C=C stretch (fluorene ring)
1375	–	1361	1361	$\text{C}_\alpha\text{-C}_\beta$ stretch (thiophene ring)
1350	1342			Bending $\text{CH}_2/\text{CH}_3$
1283	1282	1278	1284	C–C stretch + CH bend (fluorene ring)
1260	1260		1274	CH bend (fluorene ring)
1201	1226			CH bend (thiophene ring) + CH bend (fluorene ring)
	1169		1189	C–C stretch (PF-Th interring) + CH bend (fluorene ring)
1130	1118	1133	1131	Ring def. + CH bend (fluorene ring)
1090	–			Ring def. + CH bend (fluorene ring)
1017	1034	1078	1054	CH bend (thiophene ring)
880	873			“Out of plane” bending CH (fluorene)
813	828			“Out of plane” bending CH (fluorene)
794	794			“Out of plane” bending CH (thiophene)
720	723			C–S–C def. (thiophene ring)

be outlined as follows: (1) two strongly overlapping, sharp peaks at 1606 and  $1587\text{ cm}^{-1}$  can unambiguously be assigned to the aromatic C–C stretching deformations of fluorine ring, consistent with the neutral state of the copolymers; (2) three clear bands at 1490, 1446 and  $1361\text{ cm}^{-1}$  are usually attributed to the symmetric and asymmetric C=C stretching modes and the C–C stretching mode in thiophene rings respectively, [7, 19] which are also confirmed by the DFT calculations; (3) a weak band at ca. 1272 and  $1131\text{ cm}^{-1}$  are characteristic of the C–H in plane bending deformations in the fluorene ring; (4) a band pointed at  $1078\text{ cm}^{-1}$  which is always absent in 3-substituted alkylthiophene ring confirms the 2-2'-substituted thiophene rings. It should be stressed the bands from aliphatic groups are very weak in our study. In fact, Raman spectroscopy is more sensitive to vibration of conjugated and unsaturated bonds. In addition, in our experimental condition ( $\lambda_{\text{exc}} = 785\text{ nm}$ ) we were in pre-resonance with the conjugated carbon backbone. Finally, all the

assignments were confirmed by the examination of the vibration modes (Cartesian displacements) of the main modes, modeled by quantum chemical calculations.

High-resolution of the XPS survey spectra and core level peaks of C(1s), S(1s) for PDOF-*alt*-Th are presented in Fig. 3. On the survey data, C(1s), S(2s), S(2p) were pointed out, but also Si(2s), Si(2p) and O(1s) assigned to the substrate (standard microscope slide). No trace of Br(3d) and B(1s) were discernible at 68 and 186 eV respectively. The C 1s peak is composed of two components at 284.9 and 284.5 (FWHM = 0.95 eV). The first component can be assigned to the  $\text{sp}^3$  saturated hydrocarbons C-(C, H) and the second component to the addition of the  $\text{sp}^2$  aromatic carbons in fluorene and the  $\text{sp}^2$  carbon in thiophene ring. No sign of oxidation could be observed. In the S(2s) region, the peak assigned to sulphur atoms of the thiophene unit is located at 228.3 eV (FWHM = 1.8 eV). Finally, Table 2 lists the surface elemental analysis (in at%) for the polymer studied, which is compared with

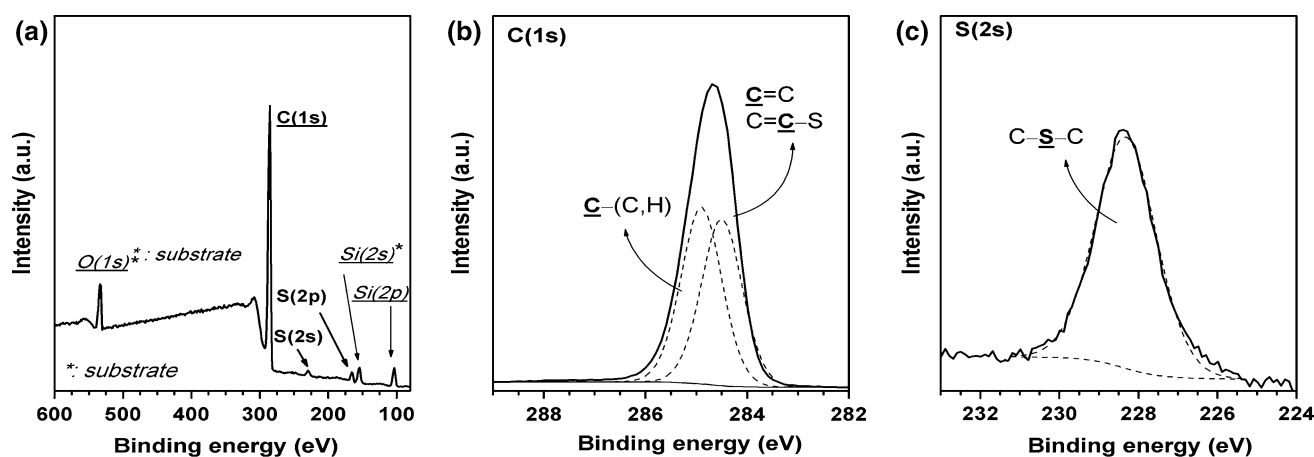


**Fig. 3** a XPS data of PDOF-*alt*-Th: a survey spectra, b C(1s) and c S(2s) core level spectra (solid lines) and curve-fitting results (shown as dashed lines)

**Table 2** XPS-determined and theoretically calculated contents in at% ( $\pm 0.4$  %) of C, S and Br in thin films of PDOF-*alt*-Th

	C 1s (aro.)	C 1s (sp <sub>3</sub> )	S 2s (thio.)	Br
Expt. (at%)	47.1	49.9	2.8	n.o. (<0.05)
Calc. (at%)	47.1	50.0	2.94	–

n.o. no observable

theoretically calculated values. The peaks of bromine and boron have not been detected, indicating synthesis and efficient removal of the oligomers. A good agreement between the determined and theoretically calculated contents of all elements in these polymers should be pointed out.

The main spectroscopic feature of conjugated polymers is an intensive absorption band with a maximum in the visible part of the spectrum. This band is usually ascribed to the  $\pi$ - $\pi^*$  transition in the conjugated backbone and is used for the calculation of optical band gap. This band gap is mainly influenced by electron donating/accepting properties of the segments constituting the polymer repeating unit and by steric factors. This applies not only to the UV-Vis absorption spectroscopy but also to photoluminescence. In Fig. 4, UV-Vis absorption and emission spectra of PDOF-*alt*-Th copolymer are presented. A broad absorption band from 300 to 480 nm and centered at 430 nm, related to the formation of PDOF-*alt*-Th copolymer was observed. By comparing with poly(9,9-dioctylfluorene) (PDOF) we observe a significant Bathochromic shift with the copolymer, induced by the addition of two lateral thiophene groups to the dioctylfluorene unit [25]. Similar trend is observed in the photoluminescence spectra. This shift can be a consequence of electron donating property of the thiophene groups which increases the electron accepting property of the copolymer, and

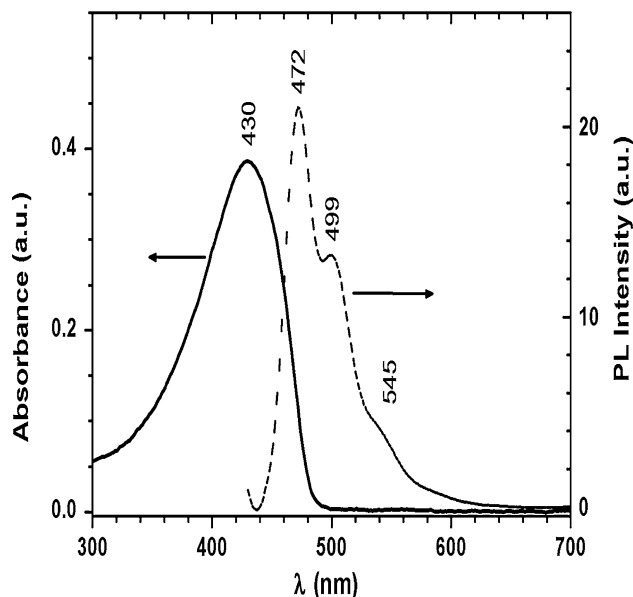


**Fig. 4** Absorption and emission spectra ( $\lambda_{\text{exc}} = 430$  nm) of poly(9,9-dioctylfluorene-*alt*-thiophene) (sample concentration was  $5.6 \cdot 10^{-6}$  g mL<sup>-1</sup>)

decreases the LUMO level of the polymer. Alternative explanation involves the conjugation caused by the presence of thiophene ring which renders the polymer chain more planar [26]. It was verified by Grova et al. [27, 28] who studied similar copolymers based on dialkylfluorene and thiophene, that these materials can absorb between 350 and 450 nm. It should be noted that the absorption onset can be used to estimate the band gap ( $E_g$ ) of the materials. A value of 2.53 eV can be found for PDOF-*alt*-Th copolymer, near the value of 2.55 eV proposed by Grova et al. [28].

The emission spectrum of the PDOF-*alt*-Th copolymer is presented Fig. 4 where the maxima are observed at 472

and 499 nm, and a shoulder at 545 nm. These peaks were attributed to the emission of polymeric materials formed from fluorene and thiophene [29]. This result shows a significant redshift of the emission compared to PDOF (peaks at 424 and 448 nm with emission in blue [30]). These results, and those observed in the absorption spectrum confirm the formation of the copolymers under investigation.

UV–Vis and photoluminescence spectra of PDOF-*alt*-Th were red-shifted in regard to PDOF, which involves the reduction of the optical band gap. However, the optical band gap indicates only that the energetic difference between the HOMO and LUMO levels in both polymers, but provides no information about the relative positions of these levels. To resolve this problem we have used electrochemical methods, and more precisely cyclic voltammetry. The position of the HOMO level, which is related to the ionization potential ( $I_p$ ) of a given polymer, can be indirectly determined from cyclic voltammetry data, assuming that the onset of the first anodic peak corresponds to the removal of an electron from the HOMO level. For the calculations of the HOMO and LUMO level (approximated by  $I_p$ ) the potentials of the oxidation peak onset must be expressed on the absolute potential scale. If the potentials are given with respect to the Ag/AgCl couple, the following empirical formula can be used:  $E_{HOMO} = -e(E_{ox\ onset} + 4.4\text{ eV})$  [31], where  $-4.4\text{ eV}$  is the potential of Ag/AgCl couple with respect to the vacuum level, and  $E_{ox\ onset}$  the first oxidation potential (V).

Three cyclic voltammograms of poly(9,9-dioctylfluorene-*alt*-thiophene) previously drop casting on platinum electrode in  $0.100\text{ mol L}^{-1}$  LiClO<sub>4</sub>/ACN versus Ag/AgCl are presented. The cyclic voltammogram recorded until  $+1.10\text{ V}$  (Fig. 5) reveals one oxidation and one reduction peak at  $+1.04$  and  $+0.88\text{ V}$ , respectively. When scanned until  $+1.40\text{ V}$ , it was observed two oxidation peaks at  $+1.04$  and  $+1.23\text{ V}$  and only one reduction peak at  $+0.85\text{ V}$ . This electrochemical behavior has been observed on thiophene compounds [16] and too observed in copolymers derived from dioctylfluorene and thiophene [28, 29, 32], so that the first oxidation peak was related to species radical cation from thiophene and the second peak probably associated to the formation of a radical cation located on the fluorine moiety. When the cyclic voltammogram was conducted until  $+1.70\text{ V}$  (Fig. 5), a third oxidation peaks were observed at  $+1.61\text{ V}$ , probably related to the formation of a dictation on the thiophene or fluorene groups. These dictations were not stable, and during the following cathodic scan cycle, no reduction wave was observed, suggesting that the high achieved potential was sufficient to completely degrade the copolymer. This fact can be confirmed by subsequent cycles without electroactive behavior.

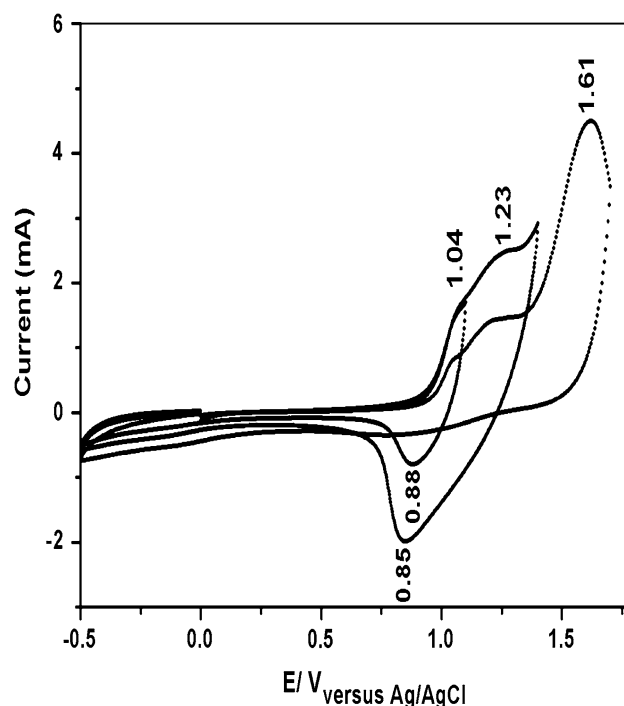


**Fig. 5** Cyclic voltammograms of PDOF-*alt*-Th copolymer in  $0.100\text{ mol L}^{-1}$  of LiClO<sub>4</sub>/ACN versus Ag/AgCl on the platinum electrode ( $\nu = 50\text{ mV s}^{-1}$ )

Considering the oxidation potentials ( $E_{ox}$ ) determined in the CV, Fig. 5, as already reported above, it was possible to define the ionization potential (IP) of the copolymer. In the voltammogram, the  $E_{ox}$  of the PDOF-*alt*-Th copolymer was  $+0.94\text{ V}$ , so the ionization potential (IP) can be obtained as  $5.34\text{ eV}$ , close to similar compounds studied [29, 32]. The LUMO levels (approximated by the electron affinity  $E_a$ ) can be estimated at  $-2.81\text{ eV}$  (derived from the following formula  $E_{LUMO} = E_{HOMO} + E_g$ ).

Figure 6 shows the Nyquist diagrams obtained by EIS in different applied potentials, which demonstrated the resistive behavior of the copolymer studied on the Pt electrode. For all Nyquist diagrams obtained in the different potentials a semicircle was observed. Two high frequency semicircles induced by the charge transport processes at the metal/polymer and polymer/solution interfaces were expected [14, 33]. However, similar to studies on these P3ATs with polydiphenylamine (PDFA) [34], only one semicircle was observed, probably due to the homogeneous non-separation of the surfaces, partial superposition of these semicircles or the characteristics of the interface processes in terms of resistance at the polymer/solution interface [15, 16].

According to the Nyquist diagrams, firstly, when potential increases an abrupt reduction of the diameter of the semicircle was occurred from  $+1.0\text{ V}$ , near the first oxidation potential peak. This observation indicates of a large change

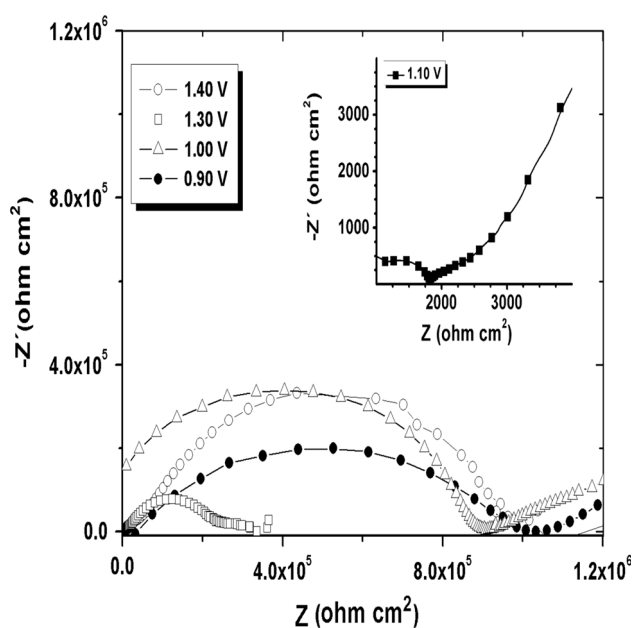


**Fig. 6** Nyquist plots obtained on different potentials for the film deposited on a platinum plate in  $0.100 \text{ mol L}^{-1} \text{ LiClO}_4/\text{ACN}$  versus  $\text{Ag}/\text{AgCl}$

in the electric resistance of the film with the introduction of radical cation in the structure. Secondly, the inverse effect was observed when the potential was increased above  $+1.3 \text{ V}$ .

In Table 3, the charge transfer resistance values ( $R_{\text{CT}}$ ) and the maximum frequency of the deposited film on platinum determined from the Nyquist diagrams are presented. A high reduction of  $R_{\text{CT}}$  was observed after the first oxidation peak ( $+1.1 \text{ V}$ ) and a rise after the second oxidation wave ( $+1.4 \text{ V}$ ). This latter increase of  $R_{\text{CT}}$ , with the application of larger potentials, confirms the absence of electroactive behavior of the copolymer as observed in CV (Fig. 3a), probably due to the beginning of the degradation process. This behavior was also observed in polyalkylthiophenes synthesized on platinum electrode and ITO [15, 16, 34].

**Table 3** Charge transfer resistance ( $R_{\text{CT}}$ ) of the film obtained from Nyquist plots at different potentials

Different potentials (V)	Maximum frequency (Hz)	$R_{\text{CT}}$ ( $\Omega$ )
0.80	$6.37 \times 10^5$	$12.1 \times 10^5$
0.90	$4.58 \times 10^5$	$9.5 \times 10^5$
1.00	$3.73 \times 10^5$	$8.9 \times 10^5$
1.10	$4.16 \times 10^2$	$6.9 \times 10^2$
1.20	$8.23 \times 10^2$	$1.4 \times 10^2$
1.30	$2.00 \times 10^3$	$4.9 \times 10^3$
1.40	$3.40 \times 10^5$	$9.8 \times 10^5$

For conjugated polymers, the spectroelectrochemistry studies can help in a more precise understanding of the electrochemical doping of copolymers. Indeed, their UV–Vis–NIR and Raman spectra are extremely sensitive to the doping process. For example in Fig. 7a, UV–Vis spectra of the PDOF-*alt*-Th copolymer obtained after electrooxydation are presented. During oxidation of the copolymer, it was observed in the spectrum the progressive bleaching of the band at  $430 \text{ nm}$ . This bleaching of the band at  $430 \text{ nm}$  is generally accompanied by an appearance and consecutive growth of two doping-induced bands with maxima in the red and near infrared range. Oxidative doping of conjugated polymers follows in general the two states model involving the formation of radical cations (polarons) in the first step and spinless dications (bipolarons) in the second one. However, in polymers showing a rather limited conjugation length and by consequence high oxidative doping potential, only the first oxidation process takes place which, then, is followed by the over oxidation. Hence, the complete disappearance of the absorption band has occurred at  $+1.70 \text{ V}$ , confirming the degradation of the film as already pointed out earlier by cyclic voltammetry.

Concerning the Raman spectroscopy, the response of PDOF-*alt*-Th as a function of the potential are presented Fig. 7b, c. The assignments of the main Raman bands have already discussed above. Having in mind these attributions, Raman spectroelectrochemistry can be analyzed. Significant changes are expected in the Raman spectra of the electrochemically doped copolymer because this process involves modifications of the chemical bonds, as a consequence of an electron removal from the HOMO level (oxidative doping). This alters the force constants of chemical bonds and leads to a shift of selected Raman bands in the spectra of doped polymers. Moreover, doping frequently induces the changes in the bond sequence (for example quinoid *vs* benzenoid) as well as in the conformation of the macromolecule. Thus, some Raman bands may disappear and new bands may appear. Accordingly, all changes in the Raman fingerprints of the copolymer can be considered as an indication of an evolution in its electronic and/or conformational structure.

In Fig. 7b, Raman spectra of PDOF-*alt*-Th, registered during the oxidation processes are depicted. From the open circuit potential up to  $E = +0.9 \text{ V}$ , no doping-induced changes are seen and all spectra remain unmodified and characteristic of the neutral state of PDOF-*alt*-Th. For instance, the main bands were observed at  $1446$  and  $1606 \text{ cm}^{-1}$ , characteristic of the symmetric stretching of the thiophene and fluorene rings, respectively. When a potential near the first oxidation peak was applied ( $+1.0 \text{ V}$ ), the intensity of the band at  $1446 \text{ cm}^{-1}$  abruptly decreases, and simultaneously a new band at  $1474 \text{ cm}^{-1}$  has appeared. It should be noted that this evolution is



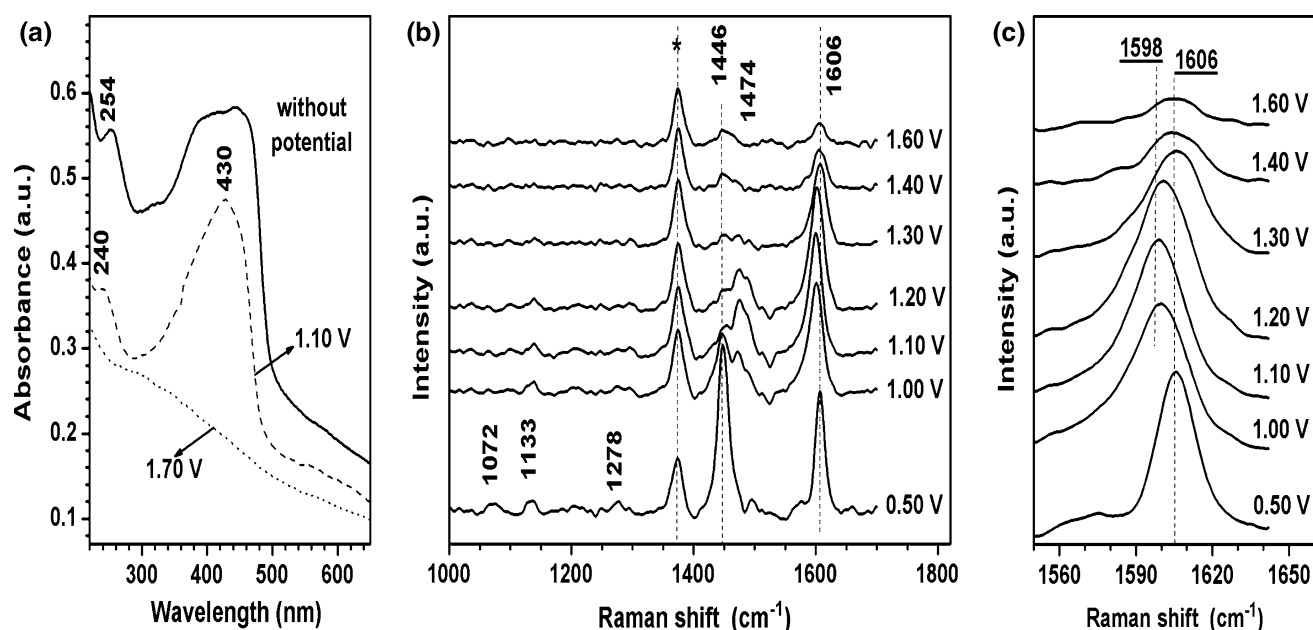


**Fig. 7** **a** UV–Vis spectra ex situ of PDOF-*alt*-Th copolymer deposited on platinum (reflection configuration), **b** in situ Raman spectra of PDOF-*alt*-Th at the different applied potentials in 0.1 M

LiClO<sub>4</sub>/ACN vs Ag/AgCl. (\*) Band related to the solvent. **c** in situ Raman spectra of PDOF-*alt*-Th at the different applied potentials in the 1560–1660 cm<sup>-1</sup> range

characteristic of the formation of radical cation and the structural modification from the aromatic to the quinoid form of the thiophene ring [16]. A shift of the band at 1606 to 1598 cm<sup>-1</sup> was also observed, due to the modification of the fluorine ring too. Thus, the reduction of the RCT of the copolymer, in potentials near the first oxidation peak is due to (1) the stabilization of quinoid structure, (2) the formation of a radical cation that favors charge transport processes involved in optoelectronic devices.

Then, for +1.3 V, a new diminution of the intensity of the bands at 1446 and 1474 cm<sup>-1</sup> was observed, whereas the band at 1598 cm<sup>-1</sup> was returned to 1606 cm<sup>-1</sup>. Finally, all these bands disappear completely when a potential of +1.60 V was applied. These results show that the copolymer degradation begins by the thiophene ring, followed by variations in the fluorene structure.

From these observations it is possible to propose the following mechanism: When the first electron is removed from the conjugated copolymer, the radical cation is mainly located on the thiophene ring as represented in Scheme 2, structure **2** (PFT<sup>•+</sup>). When a second electron is then pulled out, two structures can be proposed: the formation of a second radical cation (PFT<sup>2(•+)</sup>) located on the fluorine moiety (structure **3**, Scheme 2), or the creation of a spinless dication PFT<sup>(2+)</sup> located on the thiophene ring. This last hypothesis is unlikely, because a thiophene ring cannot support two positive charges. Finally, for higher potential, associated to the third non-reversible oxidation wave observed on Fig. 5c, the degradation of the

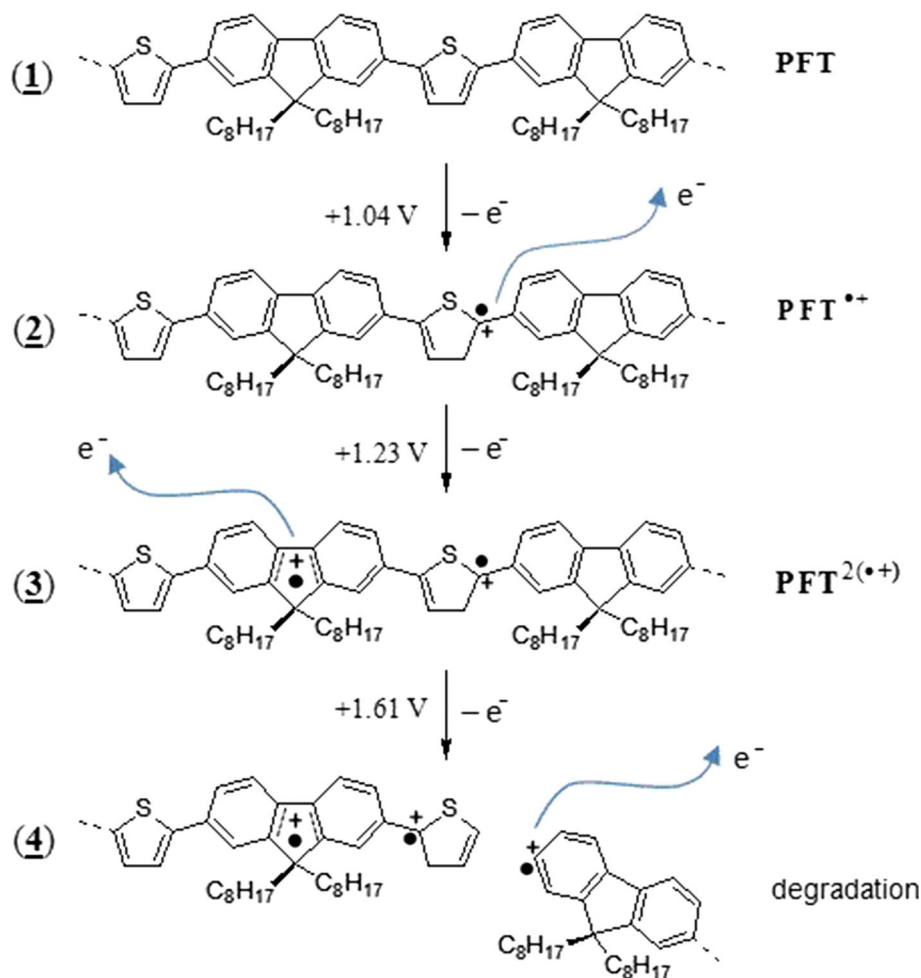
copolymer occurs, probably from the scission of the chain (structure **4**, Scheme 2).

#### 4 Conclusion

In this work, the synthesis by Suzuki reaction of an alternating copolymer of dioctylfluorene and thiophene was studied by FT-IR, Raman and XPS spectroscopies, UV–Vis absorption and photoluminescence, electrochemistry and finally spectroelectrochemistry. The main purpose was to suggest a comprehensive description of this copolymer, from its electronic and conformational structure, and to characterize its oxidative states. An attentive and deeper analysis of its vibrational spectra was done. This analysis was very important, considering the following Raman spectroelectrochemistry study. XPS analysis has confirmed that in the chemical structure of the copolymer formed there is no bromo or borone units, and the stability during the thin film process.

The knowledge of the optical absorption and the photoluminescence were crucial in our study. First, optical bandgap of the material has been estimated. Secondly, information about resonance or pre-resonance condition during the Raman investigation, and the excitation range where Raman experiments can be done, without large fluorescence has been determined. Lastly, the addition of thiophene units which has caused a redshift of the absorption and emission of the copolymer can be seen as an

**Scheme 2** Chemical structures of PDOF-*alt*-Th electrochemically oxidized to radical cations



indicator of a good conjugation and a high planarity of the neutral chain.

Concerning the study of the oxidation levels of the copolymer, different complementary techniques were used. Electrochemistry and electronic impedance spectroscopy have given information on the ionization potential ( $I_p$ ), and on the charge transfers. Through the EIS, Nyquist diagrams were registered, in which low charge transfer resistance values were observed for the copolymer when subjected to the first oxidation potential. So, with the in situ Raman technique it was possible to explain the low resistance to charge transfer of the copolymer with respect of radical cation formation in the copolymer, and we were able to propose a mechanism of oxidation of the copolymer, and on its degradation.

Finally, we believe that this study leads to important conclusions concerning the formation of radical cations and charge carriers generation in this copolymer. The accurate Raman bands analysis has lead to a better understanding of the complex mechanisms involved in the formation of the excited states of this polymer, on the

formation of charge carriers, on the modifications of the local conformation as well as on the localization of radical cations within conjugated units.

**Acknowledgments** We would like to express our appreciation of the Spectroscopy Laboratory (SPEC) at the PROPPG/Uel Multiuser Center and the work was supported by CNPq program/special visiting researcher (PVE), Process No. 401109/2014-3 and Project No. 441689/2014-0.

## References

1. T. Miteva, A. Meisel, W. Knoll, H.G. Nothofer, U. Scherf, D.C. Müller, K. Meerholz, A. Yasuda, D. Neher, *Adv. Mater. (Weinheim, Ger.)* **13**, 565 (2001)
2. L. Akcelrud, *Prog. Polym. Sci.* **28**, 875 (2003)
3. S. Günes, H. Neugebauer, N.S. Sariciftci, *Chem. Rev. (Washington, DC, US)* **107**, 1324 (2007)
4. I. Etxebarria, J. Ajuria, R. Pacios, *Org. Electron.* **19**, 34 (2015)
5. U. Scherf, D. Neher, *Polyfluorenes* (Springer, Berlin, 2008), pp. 49–84
6. A. Pron, P. Gawrys, M. Zagorska, D. Djurado, R. Demadrille, *Chem. Soc. Rev.* **39**, 2577 (2010)

7. C. Ottone, P. Berrouard, G. Louarn, S. Beaupré, D. Gendron, M. Zagorska, P. Rannou, A. Najari, S. Sadki, M. Leclerc, A. Pron, *Polym. Chem.* **3**, 2355 (2012)
8. N.A. Yamamoto, L.L. Lavery, B.F. Nowacki, I.R. Grova, G.L. Whiting, B. Krusor, L.S. Roman, *J. Phys. Chem. C* **116**, 18641 (2012)
9. B. Qu, L. Feng, H. Yang, Z. Gao, C. Gao, Z. Chen, L. Xiao, Q. Gong, *Synth. Met.* **162**, 1587 (2012)
10. C.G. Wu, M.F. Chung, H.H.G. Tsai, C.J. Tan, S.C. Chen, C.H. Chang, T.W. Shih, *ChemPlusChem* **77**, 832 (2012)
11. S. Jungstittiwong, R. Tarsang, Y. Surakhot, J. Khunchalee, T. Sudyoadsuk, V. Promarak, S. Namuangruk, *Org. Electron.* **13**, 1836 (2012)
12. Y. Fu, L. Shi, D. Zhu, C. He, D. Wen, Q. He, J. Cheng, *Sens. Actuators, B* **180**, 2 (2013)
13. N. Miyaura, A. Suzuki, *Chem. Rev. (Washington, DC, US)* **95**, 2457 (1995)
14. J.R. MacDonald, *Electrochim. Acta* **35**, 1483 (1990)
15. T.N.M. Cervantes, D.C. Bento, E.C.R. Maia, R.V. Fernandes, E. Laureto, G.J. Moore, G. Louarn, H. de Santana, *J. Mater. Sci. Mater. Electron.* **25**, 1703 (2014)
16. D.C. Bento, E.C.R. Maia, T.N.M. Cervantes, C.A. Olivati, G. Louarn, H. de Santana, *J. Mater. Sci. Mater. Electron.* **26**, 149 (2015)
17. L.O. Péres, N. Errien, E. Faulques, H. Athalin, S. Lefrant, F. Massuyeau, J. Wéry, G. Froyer, S.H. Wang, *Polymer* **48**, 98 (2007)
18. M.J. Frisch et al., *Gaussian 09, Revision A.02*, Gaussian, Inc., Wallingford CT, 2009
19. G. Louarn, J.P. Buisson, S. Lefrant, D. Fichou, *J. Phys. Chem.* **99**, 11399 (1995)
20. M. Ariu, D.G. Lidzey, D.D.C. Bradley, *Synth. Met.* **111**, 607 (2000)
21. M. Ariu, D.G. Lidzey, M. Lavrentiev, D.D.C. Bradley, M. Jandke, P. Strohmriegl, *Synth. Met.* **116**, 217 (2001)
22. I. Kulszewicz-Bajer, G. Louarn, D. Djurado, L. Skorka, M. Szymanski, J.-Y. Mevellec, S. Rols, A. Pron, *J. Phys. Chem. B* **118**, 5278 (2014)
23. G. Varsányi, *Vibrational Spectra of Benzene Derivatives* (Academic Press, New York, 1969), pp. 17–84
24. A.P. Kulkarni, Y. Zhu, S.A. Jenekhe, *Macromolecules* **38**, 1553 (2005)
25. Q. Hou, Y. Xu, W. Yang, M. Yuan, J. Peng, Y. Cao, *J. Mater. Chem.* **12**, 2887 (2002)
26. G. Vamvounis, S. Holdcroft, *Adv. Mater. (Weinheim, Ger.)* **16**, 716 (2004)
27. I.R. Grova, A.G. Macedo, L.S. Roman, L. Akcelrud, *Eur. Polym. J.* **49**, 3539 (2013)
28. I.R. Grova, D.J. Coutinho, R.M. Faria, L. Akcelrud, *J. Polym. Res.* **20**, 119 (2013)
29. V. Promarak, A. Punkvung, S. Jungstittiwong, S. Saengsuwan, T. Sudyoadsuk, T. Keawin, *Tetrahedron Lett.* **48**, 3661 (2007)
30. E. Lim, B.J. Jung, H.K. Shim, *Macromolecules* **36**, 4288 (2003)
31. L.O. Péres, M.R. Fernandes, J.R. Garcia, S.H. Wang, F.C. Nart, *Synth. Met.* **156**, 529 (2006)
32. F. Jaramillo-Isaza, M.L. Turner, *J. Mater. Chem.* **16**, 83 (2006)
33. E.M. Giroto, M.A. De Paoli, *Quim. Nova* **22**, 358 (1999)
34. D.C. Bento, E.C.R. Maia, P.R.P. Rodrigues, G. Louarn, H. De Santana, *J. Mater. Sci. Mater. Electron.* **24**, 4732 (2013)